# Conductivity mechanism analysis at high temperature in bismuth titanate: A single crystal with sillenite-type structure

S. Lanfredi and M. A. L. Nobre

Citation: Applied Physics Letters **86**, 081916 (2005); doi: 10.1063/1.1869542
View online: http://dx.doi.org/10.1063/1.1869542
View Table of Contents: http://scitation.aip.org/content/aip/journal/apl/86/8?ver=pdfcov
Published by the AIP Publishing

# Conductivity mechanism analysis at high temperature in bismuth titanate: A single crystal with sillenite-type structure

S. Lanfredi[a] and M. A. L. Nobre[a),b)]
*Faculdade de Ciências e Tecnologia—FCT, Universidade Estadual Paulista—UNESP, C. P. 467, CEP: 19060-900, Presidente Prudente—SP, Brazil*

(Received 29 November 2004; accepted 4 January 2005; published online 18 February 2005)

Conductivity behavior of the $Bi_{12}TiO_{20}$ single crystal was investigated by the electric modulus spectroscopy, which was carried out in the frequency range from 5 Hz to 13 MHz and at temperatures higher than 400 °C. The resistance curve exhibits a set of properties correlated to a negative temperature coefficient thermistor. In the temperature range investigated, the characteristic parameter ($\beta$) of the thermistor is equal to 4834 °C. Temperature coefficients of the resistance ($\alpha$) were derived being equal to $-3.02\times10^{-2}$ °$C^{-1}$ at 400 °C and equal to $-9.86\times10^{-3}$ °$C^{-1}$ at 700 °C. The nature of the electric relaxation phenomenon and magnitude dc conductivity are approached. © *2005 American Institute of Physics*. [DOI: 10.1063/1.1869542]

Bismuth titanium oxide $Bi_{12}TiO_{20}$ (BTO) crystallize on the I23 space group in a body centered cubic structure termed as sillenite.[1] This class of crystal exhibits a set of interesting physical properties, as electro-optical, elasto-optical, optical activity, photoconductivity, and piezoelectrical properties. These properties allow to the sillenite a wide range of potential technological applications, such as a reversible recording medium for real-time holography or image processing.[2,3] Recent investigations have been addressed to the analysis of optical properties of sillenite-type crystals.[1,4] The combination of the electro-optical and photoconductivity properties, from which results the so-called photorefractive effect, consists of a reversible light induced change in the refractive index.[5] However, few reports are available regarding electrical properties of the BTO crystal as a function of temperature, in specific far from room temperature.[6]

This work presents an insight on the conductivity phenomenon of the BTO single crystal as a function of temperature. A set of electrical parameters assigned to high temperature properties is derived. Analysis of these parameters indicates that the BTO electric resistance behaves as a negative temperature coefficient (NTC) thermistor. NTC thermistors are commonly polycrystalline ferrite spinels[7] with a combination of cations of transition metals or single cation phase. Recently, NTC thermistors based on the polycrystalline antimoniate with structure type spinel or pyrochlore have been reported at high temperature.[8,9] Interesting thermistor parameters have been reported for $Zn_7Sb_2O_{12}$ and $Bi_3Zn_2Sb_3O_{14}$ ceramics, which were derived from analysis of impedance spectroscopy measurements.[8–10]

$Bi_{12}TiO_{20}$ single crystal was grown by the pulling techniques, using a resistive heating furnace and pure platinum crucibles. The starting batch melt was prepared by thoroughly mixing an appropriate amount of bismuth oxide and titanium oxide, followed by melting at temperature ranging from 900 to 950 °C.

BTO seed oriented along the [001] direction, held in a pure platinum seed holder, was used to start crystal growth. Further details are described elsewhere.[6]

The electrical characterization of the BTO crystal was carried out by impedance spectroscopy on $7\times6\times3$ mm sample, which was cleaned with acetone in an ultrasonic cleaner for 5 min and dried at 100 °C. Gold electric ohmic contacts were deposited to the sample using the sputtering technique. Electric measurements were carried out in the frequency range of 5 Hz–13 MHz, with an applied potential of 500 mV, using a Solartron 1260 impedance analyzer controlled by a personal computer. A sample holder with a two-electrode configuration was used. Electric modulus $M^*(\omega)$ was derived from impedance ($Z^*(\omega)=Z'(\omega)-jZ''(\omega)$) measurements, which were carried out from 400 to 700 °C with a 50 °C temperature step. A 30 min interval was adopted prior to the thermal stabilization of the sample after each measuring temperature. All the measurements were performed in atmospheric air. None kind of thermal hysteresis was observed in the measuring performed during a heating and cooling cycle. An electrical analysis derived from electric modulus gives further insight into the conductivity relaxation. The electric modulus $M^*(\omega)$ was used as further tool to the conduction relaxation analysis.[11–13] The electric modulus formalism is given by the relation $M^*(\omega)=j\omega C_0 Z^*(\omega)=M'(\omega)+jM''(\omega)$, where $C_0$ is the vacuum capacitance of the cell, $\omega$ is the angular frequency ($2\pi f$). Figure 1 shows normalized-imaginary parts $M''/M''_{\max}$ of the electric modulus as a function of logarithmic frequency for BTO at several temperatures. According to Fig. 1, the $M''/M''_{\max}$ curve exhibits a maximum with a slight asymmetry. All peaks shift toward more high frequencies with increasing measurement temperature. The electric relaxation observed is a thermally activated process.

Figures 2(a) and 2(b) show the variation of normalized parameters $\tan\delta/\tan\delta_{\max}$, $M''/M''_{\max}$ and $Z''/Z''_{\max}$ as a function of logarithmic frequency measured at 400 and 600 °C, respectively.

All three normalized parameters should be considered simultaneously prior to discerning between localized (short range conduction associated with dielectric relaxation) and non-localized (long range) conduction. According to Fig. 2,

a)Members of the UNESP/CVMat - Virtual Center of Research in Materials.
b)Author to whom correspondence should be addressed; electronic mail: nobremal@prudente.unesp.br



 

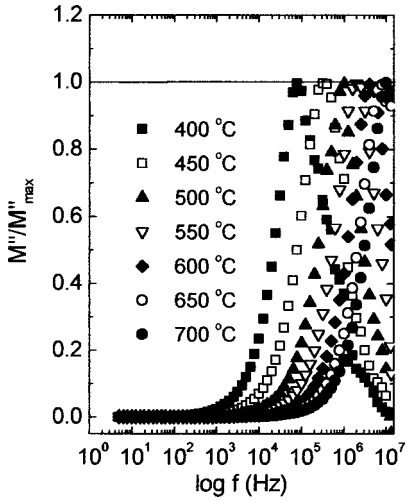


FIG. 1. Normalized-imaginary parts $M''/M''_{\max}$ of the electric modulus as a function of logarithmic frequency for $Bi_{12}TiO_{20}$ at several temperatures.

there is an overlapping of peaks of $Z''/Z''_{\max}$ and $M''/M''_{\max}$. Such development is evidence of long-range conductivity.[11,13] Thus, a dc conductivity contribution can be expected at frequencies up to the peak frequency, according

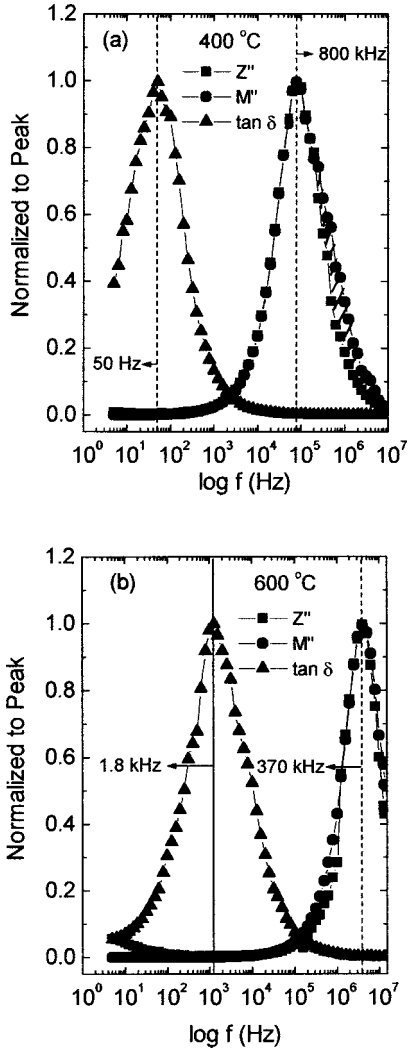


FIG. 2. Variation of normalized parameters $\tan\delta/\tan\delta_{\max}$, $M''/M''_{\max}$ and $Z''/Z''_{\max}$ as a function of logarithmic frequency measured at: (a) 400 and (b) 600 °C.

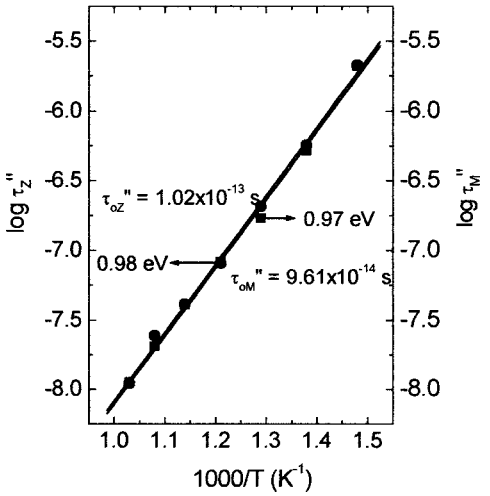


FIG. 3. Logarithmic of relaxation times, derived from $Z''$ and $M''$ functions, as a function of reciprocal temperature $1/T$.

to Figs. 1, 2(a), and 2(b). However, an asymmetric character of peaks at frequencies above maximum frequency suggests further contribution of the lattice defect or structural aspects to the conduction relaxation. Furthermore, three peaks that describe *a priori* the same relaxation process[11–13] are in complete accordance with following order proposed elsewhere.[13]

$$\tau_{\tan\delta} > \tau_Z \geqslant \tau_M, \tag{1}$$

where $\tau$ is the relaxation time and the subscripts represent the loss tangent $(\tan\delta)$, $Z$ the complex functions $Z^*(\omega)$, and $M$ the $M^*(\omega)$. The experimental verification of relation (1) suggests that long range conductivity is the major contribution at conductivity process at frequency and temperature range investigated.

The logarithmic of relaxation times, derived from $Z''$ and $M''$ functions, as a function of reciprocal temperature $1/T$, are shown in Fig. 3. The derived data are described by Arrhenius' law:

$$\tau_g = \tau_0 \exp(E_{a\tau}/kT), \tag{2}$$

where $\tau_0$ is the preexponential factor or characteristic relaxation time constant and $E_{a\tau}$ is the activation energy for the conduction relaxation. The relaxation time is a thermally activated process. The activation energy values of $E_{a\tau Z''}$ and $E_{a\tau M''}$ obtained are similar, being equal to 0.98 and 0.97 eV, respectively. These values are very similar to the $E_{a\sigma}$ calculated from conductivity data, which are in the range 0.99–1.06 eV.[6,14]

Such level of accordance between $E_\sigma$, $E_{a\tau Z''}$, and $E_{a\tau M''}$ indicates actuating of a single electronic conduction mechanism. Both $\tau_0$ values derived from $\tau_{Z''}$ and $\tau_{M''}$ parameters are of the order of $10^{-13}$–$10^{-14}$ s being compatible with phenomenon correlated to the defect lattice vibration frequency.[8] In the BTO, the $Ti^{+4}$ cation is tetrahedrally coordinated, occupying the cube corners and body-centered sites and linked by hepta-coordinated bismuth atoms. In fact, the Ti-vacancy complex has been suggested.[15] Taking into account that the anion sublattice is fully occupied and the oxygen is relatively immobile in the structure, most of the charge carried is electronic[16,17] and correlated to the complex defect formed by the $(Bi_{Ti}^{3+} + h_0^+)$ pair.[18]

Figure 4 shows the resistance and the logarithmic of resistance curves of $Bi_{12}TiO_{20}$ as a function of temperature.

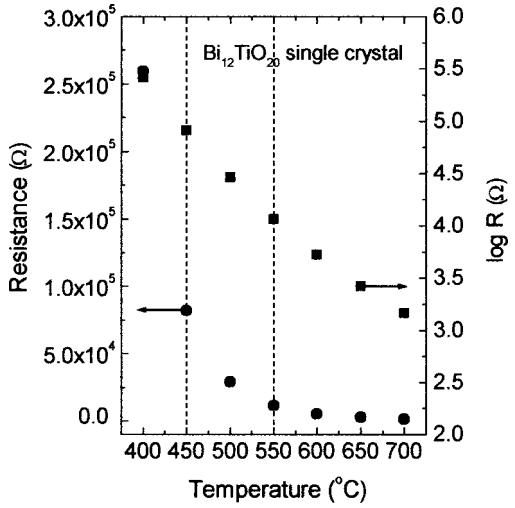


FIG. 4. Resistance and the logarithmic of resistance curves of $Bi_{12}TiO_{20}$ as a function of temperature.

The $\log R$ vs $T$ shows a linear behavior which is characteristic of a single conduction mechanism. The resistance evolution is characterized by strong temperature dependence with exponential behavior. This feature is compatible with a process of charge transfer by hopping between localized states near to the top of the valence band or to the botton of the conduction band.[19] The evolution of the resistance as a function of temperature is further characteristic of a thermistor material with a NTC. The relation between resistance and temperature for a NTC thermistor is expressed by

$$R_T = R_N \exp\left[\beta\left(\frac{T_N - T}{TT_N}\right)\right], \tag{3}$$

where $R_T$ is the resistance at temperature $T$, $R_N$ is the resistance at temperature $T_N$ known, and $\beta$ is a thermistor characteristic parameter. From Eq. (3), $\beta$ can be derived as follows:

$$\beta = [TT_N/(T_N - T)]\ln(R_T/R_N). \tag{4}$$

The sensitivity of the thermistor is defined by the temperature coefficient of resistance $\alpha$, which can be derived as a function of the $\beta$ parameter, according to the following:

$$\alpha = (1/R)[d(R)/dT] = -\beta/T^2. \tag{5}$$

Considering Fig. 4, resistance as a function of temperature curve, $\beta$ parameter was calculated by Eq. (4). The $\beta$ value calculated in the temperature range from 400 to 700 °C is equal to 4834 °C. The $\alpha$ parameter derived at 400 and at 700 °C is equal to $-3.02\times10^{-2}$ and $-9.86\times10^{-3}\,°C^{-1}$, respectively. As a whole, thermistor parameters derived and conductivity behavior are compatible with the conduction mechanism actuating on the $Bi_{12}TiO_{20}$ that is of the hopping type, in accord with defects reported previously.[16–19] From high temperature impedance measurements, the conductivity value extrapolated at room temperature equal to $1.2\times10^{-15}(\Omega\,\mathrm{cm})^{-1}$ has been reported.[8] This value is in accordance with one $[7.6\times10^{-15}(\Omega\,\mathrm{cm})^{-1}]$ reported previously at room temperature obtained via dark conductivity measurement.[14] However, at temperature range investigated, a high level of dc conductivity is detected that might be assigned to the thermal activation of a specific defect center and/or changing of the gap structure. The extrapolation of the dc conductivity at room temperature shows an unrealistic value equal to $9\times10^{-10}(\Omega\,\mathrm{cm})^{-1}$.

This work was supported by Brazilian research funding institutions FAPESP, CAPES, and CNPq.

[1] L. Arizmendi, J. M. Cabrera, and F. Agulló-López, Int. J. Optoelectron. **7**, 149 (1992).
[2] C. Zaldo, C. Coya, J. L. Fierro, K. Polgár, L. Kovács, and Zs. Szaller, J. Phys. Chem. Solids **57**, 1667 (1996).
[3] C. Coya, C. Zaldo, V. V. Volkov, A. V. Egorysheva, K. Polgár, and A. Péter, J. Opt. Soc. Am. B **13**, 908 (1996).
[4] K. Buse, Appl. Phys. B: Lasers Opt. **64**, 391 (1997).
[5] K. Buse, Appl. Phys. B: Lasers Opt. **64**, 273 (1997).
[6] S. Lanfredi, J. F. Carvalho, and A. C. Hernandes, J. Appl. Phys. **88**, 283 (2000).
[7] J. G. Fagan and V. R. W. Amarakoon, Am. Ceram. Soc. Bull. **72**, 69 (1993).
[8] M. A. L. Nobre and S. Lanfredi, J. Appl. Phys. **93**, 5576 (2003).
[9] M. A. L. Nobre and S. Lanfredi, Appl. Phys. Lett. **82**, 2284 (2003).
[10] M. A. L. Nobre and S. Lanfredi, Appl. Phys. Lett. **81**, 451 (2002).
[11] R. Gerhardt, J. Phys. Chem. Solids **55**, 1491 (1994).
[12] M. A. L. Nobre and S. Lanfredi, J. Phys. Chem. Solids **64**, 2457 (2003).
[13] W. Cao and R. Gerhardt, Solid State Ionics **42**, 213 (1990).
[14] V. Marinova, S. H. Lin, V. Sainov, M. Gospodinov, and K. Y. Hsu, J. Opt. A, Pure Appl. Opt. **5**, S500 (2003).
[15] S. H. M. Efendiev, V. E. Bagiev, A. C. H. Zeinally, V. A. Balashov, V. A. Lomonov, and A. A. Majer, Phys. Status Solidi A **63**, K19 (1981).
[16] J. A. Kilner, J. Drennan, P. Dennis, and B. C. H. Steele, Solid State Ionics **5**, 527 (1981).
[17] S. L. Hou, R. R. Lauer, and R. E. Aldrich, J. Appl. Phys. **44**, 2652 (1973).
[18] R. Oberschmid, Phys. Status Solidi A **89**, 263 (1985).
[19] V. Marinova, V. Sainov, S. H. Lin, and K. Y. Hsu, Jpn. J. Appl. Phys., Part 1 **41**, 1860 (2002).